Macromolecules **1995,** *28,* 1859–1871

Scaling Theory of Polyelectrolyte Solutions

Andrey V. Dobrynin

Department of Physics and Astronomy, University of Rochester, Rochester, New York 14627

Ralph H. Colby and Michael Rubinstein*

Imaging Research and Advanced Development, Eastman Kodak Company,
Rochester, New York 14650-2109

Received May 24, 1994; Revised Manuscript Received December 9, 1994®

ABSTRACT: We extend and generalize the scaling picture of de Gennes et al. and Pfeuty to both unentangled and entangled regimes of intrinsically flexible polyelectrolyte solutions. In semidilute solution the electrostatic persistence length of a polyelectrolyte is assumed to be proportional to the Debye screening length. If the salt concentration is low, the unentangled semidilute concentration regime spans three to four decades in polymer concentration. In this regime the dynamics of the chain is Rouse-like with viscosity weakly increasing with concentration $\eta \sim c^{1/2}$ (Fuoss law), relaxation time decreasing with concentration $\tau_{\rm Rouse} \sim c^{-1/2}$, and diffusion coefficient independent of concentration. Polyelectrolytes should form entanglements at the same relative viscosity as neutral polymer solutions ($\eta \cong 50\eta_s$). In the entangled regime of salt-free polyelectrolytes we predict the viscosity $\eta \sim c^{3/2}$, relaxation time to be independent of concentration, and diffusion coefficient $D_{\rm self} \sim c^{-1/2}$. Our predictions are found to compare favorably with experiments.

1. Introduction

Polyelectrolytes are polymers with ionizable groups.[1-8] Under appropriate conditions, such as in aqueous solutions, these groups dissociate, leaving ions on the chain and counterions in the solution. Examples of polyelectrolytes include a variety of natural polymers (biopolymers) as well as synthetic polymers that are often made water soluble by covalently bonding salts to the polymer.[1-8]

Polyelectrolyte solutions have a number of properties remarkably different from solutions of uncharged polymers. In particular:

(i) The viscosity η of polyelectrolyte solutions at low concentrations is proportional to the square root of polymer concentration $\eta \sim c^{1/2}$ (Fuoss law),[9] while for solutions of uncharged polymers at the same concentration, viscosity is proportional to concentration. There is no regime of concentration where solutions of uncharged polymers have $\eta \sim c^{1/2}$.

(ii) There is a well-pronounced peak in the scattering function of homogeneous polyelectrolyte solutions.[10,11] The wave vector corresponding to this peak increases with concentration as $c^{1/2}$. Solutions of uncharged polymers have no such peak.

(iii) At low salt concentration the main contribution to the osmotic pressure of polyelectrolyte solutions comes from counterions.[1,9]

Considerable theoretical work[12-23] has been devoted to polyelectrolyte solutions, starting from the pioneering works of Katchalsky et al.[12,13] and the scaling theory of de Gennes et al.[14] and Pfeuty.[15] A significant fraction of recent work on polyelectrolyte solutions was influenced by the ideas of electrostatic persistence length put forward by Odijk[21] and independently by Skolnick and Fixman[22] (OSF). They estimated the energy required to bend a straight charged chain and found that the screened Coulomb interactions led to very high induced stiffness. The OSF perturbation calculations[21,22] predicted that the electrostatic persistence length is proportional to the square of the Debye screening length.

Recently, Barrat and Joanny[23] proved that intrinsically flexible chains stay flexible on small length scales. They have demonstrated that for intrinsically flexible polymer the Odijk perturbation approach of bending a straight line is unstable to short wavelength fluctuations. This result is consistent with the de Gennes et al.[14] picture of electrostatic blobs inside which the Coulomb repulsion is not sufficient to deform the chain. If the Debye screening length is much larger than these electrostatic blobs, Coulomb repulsion stretches the chain of these blobs into a straight stiff cylinder.[18] Repeating the Odijk bending calculation for this cylinder of electrostatic blobs interacting via screened Coulomb potential does not qualitatively alter his original result: the electrostatic persistence length is proportional to the square of the Debye screening length. Monte Carlo simulations of a single intrinsically flexible polymer with charges interacting by screened Coulomb potential are consistent with chains being flexible on small length scales[24-27] and support proportionality of the electrostatic persistence length to the square of the Debye screening length,[24-26] as predicted by OSF.[21,22]

However, several computer simulations[28-30] indicate that a polyelectrolyte chain surrounded by ions has a much shorter electrostatic persistence length than the same chain with charges interacting via screened Coulomb potential, with the screening length calculated from the Debye–Hückel theory. These simulations clearly indicate that the distribution of ions surrounding the polymer is perturbed much more than one would expect from the Debye–Hückel theory. This leads to stronger screening of the electrostatic repulsion of charges on the chain and to a shorter electrostatic persistence length. These simulations also suggest a weaker dependence of the electrostatic persistence length on salt concentration. Similar trends were observed in the numerical solutions of the Poisson–Boltzmann equation by Le Bret[31] and Fixman.[32] The electrostatic persistence length is proportional to the Debye screening length over a wide range of concentrations rather than to the square of the Debye length as predicted by OSF.[21,22]

® Abstract published in *Advance ACS Abstracts,* February 1, 1995.

0024-9297/95/2228-1859$09.00/0

Even more importantly, experiments show that the electrostatic persistence length is proportional to the Debye screening length over three decades of salt concentration, as clearly demonstrated in the review by Tricot.[33] Therefore we assume that the effective persistence length of the chain is proportional to the electrostatic screening length and develop a simple scaling model of polyelectrolyte solutions. The same assumption was made in the scaling models of de Gennes et al.[14] and Pfeuty.[15] In this paper we generalize these scaling models and extend them to the dynamic scaling in both unentangled and entangled polyelectrolyte solutions.

In sections 2 and 3 we review the scaling picture of de Gennes et al.[14] and Pfeuty[15] for the conformation of a polyelectrolyte chain in a salt-free solution and in the presence of salt, respectively. The osmotic pressure and scattering are discussed in section 4. The dynamic properties of polyelectrolyte solutions such as diffusion coefficient, relaxation time, and viscosity are predicted in section 5. We demonstrate that the unentangled semidilute regime of polyelectrolytes covers three to four decades in polymer concentration in low-salt solutions. Therefore, the dynamics in this regime is Rouse-like and we predict that the viscosity should grow as the square root of polymer concentration $\eta \sim c^{1/2}$ (Fuoss law). Entanglement formation in polyelectrolyte solutions and predictions of dynamics in the entangled regime are also discussed in section 5. We compare our scaling theory with experiments in section 6 and find good quantitative agreement. Appendix A is a list of symbols and Appendix B discusses electrostatic screening.

2. Salt-Free Polyelectrolyte Solutions

In this section we review the scaling models of de Gennes et al.[14] and Pfeuty[15] for the configuration of a flexible polyelectrolyte in a solution with no added salt. We also utilize the collapse ideas of Khokhlov[34] to treat the case of a poor solvent for the uncharged chain.

2.1. Dilute Solution. Let us consider a polyelectrolyte solution (with c monomers per unit volume) of charged flexible chains with a degree of polymerization N and a monomer size b. For simplicity, we limit our consideration to monovalent charges on the chains and monovalent counterions. The average number of monomers between charges is A, so that the total charge on a chain is N/A. Note that A is the number of monomers between effective charges and thus incorporates any effects of counterion condensation.[2,35,36]

In a very dilute salt-free solution the counterions are homogeneously distributed throughout the system volume, because the Debye screening length is much larger than the distance between chains. Therefore, the charges on the chain interact via the unscreened Coulomb potential. The conformation of macromolecules is extended because of this interaction and the mean square end-to-end distance is proportional to the polymerization index N.[14,18] Each macromolecule in this regime can be represented as a chain of electrostatic blobs (see Figure 1), with the statistics of the chain inside the blob determined by the thermodynamic interaction between uncharged polymer and solvent. In good and Θ-solvents for the uncharged polymer the total energy of the electrostatic interaction between charges inside the electrostatic blob is of the order of the thermal energy[14,18]

$$(g_e/A)^2 e^2/(\epsilon D) \approx kT \qquad T \geq \Theta \tag{1}$$

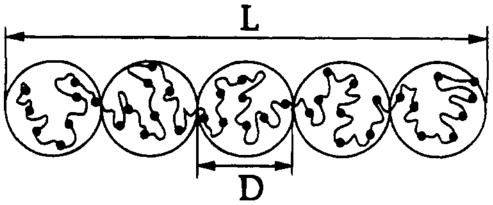

Figure 1. Polyelectrolyte chain in dilute salt-free solution. Filled circles are charged groups. The chain is an extended (rodlike) configuration of electrostatic blobs.

The number of monomers inside an electrostatic blob is g_e (g_e/A charges per blob), e is the elementary charge, ϵ is the dielectric constant of the solvent, and D is the electrostatic blob size. For the poor solvent the electrostatic blob size D is determined from a balance between the electrostatic energy of a blob and the polymer/solvent interfacial energy[34]

$$(g_e/A)^2 e^2/(\epsilon D) \approx \gamma D^2 \qquad T < \Theta \tag{2}$$

The interfacial tension is $\gamma \approx \tau^2 kT/b^2$, where $\tau \equiv (\Theta - T)/\Theta$ is the reduced temperature. The conformation of a macromolecule inside the electrostatic blob is almost unperturbed by the electrostatic interaction and depends on the quality of the solvent for the neutral polymer. Therefore, the size of the electrostatic blob is

$$D \approx b \begin{cases} (g_e/\tau)^{1/3} & T < \Theta \\ g_e^{1/2} & T = \Theta \\ g_e^{3/5} & T \gg \Theta \end{cases} \tag{3}$$

From eqs 1–3 one finds the number of monomers inside the electrostatic blob.

$$g_e \approx \begin{cases} (A^2/u)\tau & T < \Theta \\ (A^2/u)^{2/3} & T = \Theta \\ (A^2/u)^{5/7} & T \gg \Theta \end{cases} \tag{4}$$

where we have introduced a dimensionless parameter

$$u = l_B/b = e^2/(b\epsilon kT) \tag{5}$$

The Bjerrum length $l_B = e^2/(\epsilon kT)$ is the distance at which the energy of the Coulomb interaction between two elementary charges is equal to the thermal energy kT.[37] The size of the electrostatic blobs is

$$D \approx b \begin{cases} (A^2/u)^{1/3} & T \leq \Theta \\ (A^2/u)^{3/7} & T \gg \Theta \end{cases} \tag{6}$$

On length scales larger than D, electrostatics dominate and the blobs repel each other to form a fully extended chain of electrostatic blobs of length

$$L \approx DN/g_e \approx Nb \begin{cases} (u/A^2)^{2/3}\tau^{-1} & T < \Theta \\ (u/A^2)^{1/3} & T = \Theta \\ (u/A^2)^{2/7} & T \gg \Theta \end{cases} \tag{7}$$

Notice that the effect of solvent quality is merely to change the electrostatic blob, and the conformation of the chain is always a rodlike assembly of electrostatic blobs ($u/A^2 < 1$ always).

We can define parameter B as the ratio of the chain contour length Nb and the actual extended size L

$$B \equiv Nb/L = bg_e/D \approx \begin{cases} (A^2/u)^{2/3}\tau & T < \Theta \\ (A^2/u)^{1/3} & T = \Theta \\ (A^2/u)^{2/7} & T \gg \Theta \end{cases} \tag{8}$$

This parameter B depends on the quality of the solvent and controls the size and number of monomers in an electrostatic blob.

2.2. Electrostatic Screening and Overlap Concentration. Screening of electrostatic interactions in electrolyte solution is usually discussed in terms of the mean-field Debye-Hückel theory.[38] Imagine inserting a probe charge into an electrolyte solution. The length scale over which the presence of this extra charge is felt is the Debye electrostatic screening length. The Debye screening length is determined by the Bjerrum length and the number density c_i of the ions of type i carrying the charge $z_i e$

$$r_D = (4\pi l_B \sum_i c_i z_i^2)^{-1/2} \tag{9}$$

where the summation is carried out over all charges in the system.

A standard assumption in the literature is to calculate the length scale for electrostatic interaction as the Debye length caused by uncondensed (free) counterions of density c/A (we assume that counterions are monovalent $|z_i| = 1$)

$$r_D = (4\pi l_B c/A)^{-1/2} \tag{9a}$$

However, in polyelectrolyte solutions, the mean-field arguments leading to eq 9a break down in many cases, as discussed in Appendix B.

In a salt-free solution at very low polyelectrolyte concentration the Debye screening length r_D is larger than the distance between macromolecules $R_{cm} \approx (N/c)^{1/3}$ and chains are strongly interacting at concentrations below the "interaction" concentration (where $r_D = R_{cm}$).

$$c_{int} \approx [A/(4\pi u)]^3 b^{-3} N^{-2} \tag{10}$$

We shall demonstrate below that polyelectrolyte chains in a dilute salt-free solution are always extended with their end-to-end distance $R \approx L$ (eq 7). Therefore, at the overlap concentration of the salt-free solution, the distance between chains R_{cm} is equal to their extended size L:

$$c^* \approx N/L^3 \approx B^3 b^{-3} N^{-2} \tag{11}$$

Note that both the concentrations c_{int} and c^* are in the same concentration range (of order $N^{-2}b^{-3}$). For concentrations lower than both c_{int} and c^*, the Debye screening length provides the length scale for electrostatic interaction. However, at higher concentrations the electrostatic screening length is no longer given by eq 9 (see Appendix B). We distinguish three cases for electrostatic screening based on the relation of concentrations c^* and c_{int} (on the relation between parameters B and $A/(4\pi u)$).

(i) The case usually observed experimentally is where the overlap concentration is larger than the interaction concentration of the polyion lattice ($c^* > c_{int}$). In the concentration range $c_{int} < c < c^*$, the Debye screening length (r_D, eq 9a) is shorter than the distance between the dilute chains (R_{cm}). If the Debye length was the effective electrostatic screening length for $c_{int} < c < c^*$, the counterions would be localized within r_D of the chain, leaving the space between the Debye spheres practically free of counterions. Therefore, in salt-free solutions the screening length $r_D < R_{cm}$ would lead to a prohibitively large entropic penalty. In Appendix B we show that the Debye–Hückel approximation is violated in this case and argue that the shortest possible electrostatic screening length r_{scr} in salt-free solutions for $c_{int} < c < c^*$ is the distance between chains

$$r_{scr} \approx R_{cm} \approx (N/c)^{1/3} \qquad c_{int} < c < c^* \tag{12}$$

At the overlap concentration this electrostatic screening length is simply the chain size $r_{scr}(c^*) = L$. In Appendix B we postulate that above c^* the electrostatic screening length r_B has the same concentration scaling as the Debye length r_D but is larger ($r_B > r_D$).

$$r_B \approx L(c/c^*)^{-1/2} \approx (B/bc)^{1/2} \qquad c > c^* \tag{13}$$

because $c^* \approx N/L^3 \approx B/(bL^2)$.

(ii) The case of $c^* < c_{int}$ implies a semidilute concentration range $c^* < c < c_{int}$ where polyelectrolytes are strongly interacting. While this case is much less frequent (case i is the usual one), it is nonetheless possible and is also considered in Appendix B. Like case i, we conjecture the effective electrostatic screening length in semidilute solution to be proportional to the Debye length, but in this case is smaller than r_D.

(iii) Since both the overlap concentration c^* and the interaction concentration c_{int} have the same dependence on the degree of polymerization $c^* \sim c_{int} \sim N^{-2}$, there is a special point in the parameter space for polyelectrolyte solutions ($B = A/4\pi u$) at which $c^* = c_{int}$. The scaling characteristics of the chain do not depend on the quality of the solvent for the neutral polymer, and the electrostatic interactions are screened at the Debye length for all concentrations of polyelectrolyte.

Thus for all cases eq 13 provides the electrostatic screening length, in semidilute solution, with parameter B defined by eq 8. We will see in the section 6 that experiments correspond to case i ($c_{int} < c^*$), with eq 8 providing a reasonable estimate of the relations among A, B, and u.

In Appendix B we argue that the behavior of the chain in the cases i and ii results in an effective electrostatic screening length at c^* that is equal to the chain size. This condition effectively determines the parameter B, and the electrostatic screening length in semidilute solution is given by eq 13. We turn our attention below to a semidilute solution. Due to the rodlike conformation of the polyelectrolyte chain, c^* and c_{int} are very low ($\sim N^{-2}$) and the semidilute regime is very important.

2.3. Semidilute Solution. The major feature of a semidilute solution ($c > c^*$) is the existence of the correlation length[39] ξ. On length scales smaller than the correlation length, the dilute solution scaling applies. On longer length scales the chain is a random walk. At the overlap concentration c^* the correlation length is of the order of the chain size L in dilute solution. The scaling assumption[39] is that the correlation length ξ has a power law concentration dependence for $c > c^*$.

$$\xi \approx L(c/c^*)^m \tag{14}$$

The exponent m is determined from the condition that the correlation length does not depend on the degree of

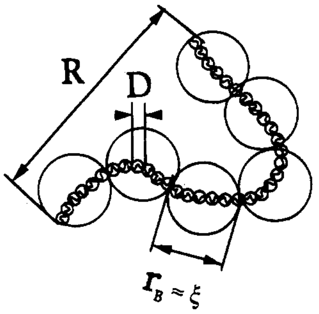

Figure 2. Polyelectrolyte chain in semidilute salt-free solution. The chain is a random walk of correlation blobs, each of which is an extended configuration of electrostatic blobs.

polymerization N. From the molecular weight dependences of the overlap concentration $c^* \sim N^{-2}$ (eq 11) and the dilute chain size $L \sim N$ (eq 7), we find the exponent $m = -1/2$ and the screening length

$$\xi \approx (B/cb)^{1/2} \qquad (15)$$

Note that the correlation length ξ (eq 15) and the electrostatic screening length r_B (eq 13) are identical to within a prefactor when there is no added salt. The number of monomers g in the correlation blob of volume ξ^3 is determined from the fact that these blobs are space-filling

$$g = c\xi^3 = (B/b)^{3/2}c^{-1/2} \qquad (16)$$

As discussed in the Introduction, we assume that a polyelectrolyte becomes flexible on length scales beyond the electrostatic screening length. Therefore all interactions are screened on length scales larger than the correlation length ($r > \xi$), and the chain is a random walk of blobs with end-to-end distance

$$R \approx \xi(N/g)^{1/2} \approx (b/B)^{1/4}N^{1/2}c^{-1/4} \approx L(c/c^*)^{-1/4} \qquad (17)$$

The concentration dependence of the size of a polyelectrolyte chain in the semidilute regime ($R \sim c^{-1/4}$) is much stronger than that for a neutral polymer ($R \sim c^{-1/8}$). This scaling law was derived in the pioneering work of de Gennes et al.[14] In the semidilute salt-free polyelectrolyte solution there are three different regimes of the chain statistics, as sketched in Figure 2:

(a) $r < D$: Thermal energy dominates over electrostatics and the conformation is similar to a neutral polymer (collapsed in poor solvent; random walk in Θ-solvent; self-avoiding walk in good solvent).

(b) $D < r < \xi$: Electrostatics dominate and the chain is a fully extended conformation of electrostatic blobs.

(c) $r > \xi$: The electrostatic interactions are screened beyond $r_B \approx \xi$ and the chain is a random walk of correlation blobs.

When the polymer concentration increases even further, so that

$$c > c_D \approx b^{-3}\begin{cases} 1 & T \ll \Theta \\ B^{-1} & T = \Theta \\ B^{-2} & T \gg \Theta \end{cases} \qquad (18)$$

the screening radius becomes of the order of the electrostatic blob size D. The concept of electrostatic blob cannot be used as these high concentrations, and the screening of Coulomb interaction is mainly caused by the polymeric nature of the polyelectrolyte solution. This concentration regime was investigated in refs 40 and 41.

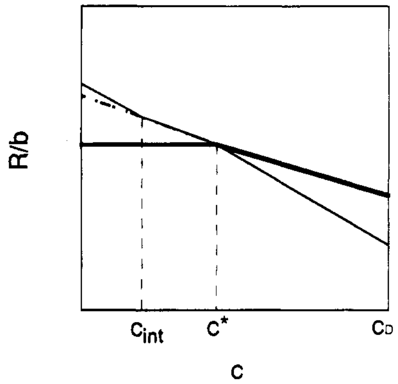

Figure 3. Concentration dependence of length scales for salt-free polyelectrolyte solutions. Thick solid lines are the end-to-end distance R ($R = L \sim c^0$ for $c < c^*$; $R \sim c^{-1/4}$ for $c > c^*$). The thin solid is the electrostatic screening length ($r_D \sim c^{-1/2}$ for $c < c_{int}$, $r_{scr} \sim c^{-1/3}$ for $c_{int} < c < c^*$, and $r_B \approx \xi \sim c^{-1/2}$ for $c > c^*$). The dash-dotted line is the distance between chains in dilute solution ($R_{cm} \sim c^{-1/3}$).

We now summarize our results for a salt-free polyelectrolyte solution by plotting the concentration dependence of different length scales (Figure 3). The dash-dotted line in Figure 3 is the average distance between macromolecules ($R_{cm} \sim c^{-1/3}$). The thin solid line is the Debye length r_D in dilute solution below the interaction concentration of the polyion lattice ($c < c_{int}$). In the concentration range $c_{int} < c < c^*$ the electrostatic screening length is of the order of the distance between polyions $r_{scr} \approx R_{cm} \sim c^{-1/3}$. The thin solid line for $c > c^*$ is the electrostatic screening length $r_B \sim c^{-1/2}$, which is proportional to the correlation length ($\xi \sim c^{-1/2}$) in a semidilute solution. The thick solid line is the root mean square chain size R in different concentration regimes. We briefly summarize all possible regimes of a salt-free polyelectrolyte solution using Figure 3:

1. $c < c_{int}$: Dilute solution of strongly interacting chains.[14] The electrostatic screening length is the Debye length, which is larger than the distance between chains ($r_D > R_{cm}$). For sulfonated polystyrene of molar mass 690 000 in water, $c_{int} \approx 4 \times 10^{-8}$ M, which is far below ordinary experimental concentrations.

2. $c_{int} < c < c^*$: Dilute solution of weakly interacting chains. The electrostatic screening length is the distance between chains ($r_{scr} \approx R_{cm}$). The polymer conformation is that of an extended chain ($R < r_{scr}$) of electrostatic blobs (eq 7 and Figure 1) for all $c < c^*$.

3. $c^* < c < c_D$: Semidilute solution ($R_{cm} < R$) of flexible chains ($R > r_B$) that are random walks of correlation of blobs (eq 17). The electrostatic screening length is proportional to, but larger than, the Debye length.

4. $c > c_D$: In this regime polyions contribute to the electrostatic screening. We estimate c_D to be a rather high concentration and will not discuss this regime any further in the present paper (see refs 40 and 41).

3. Polyelectrolyte Solutions in the Presence of Salt

In this section we consider the behavior of a polyelectrolyte solution in the presence of salt (e.g., 1–1 electrolyte with concentration c_s far below its saturation concentration). At very low polyelectrolyte concentrations ($c < c_{int}$) the Coulomb interactions between charged monomers are screened by both counterions and salt ions. The Debye screening length r_D is determined from eq 9 with number density c/A for counterions and $c_{s+} = c_{s-} = c_s$ for positive and negative salt ions (with all $|z_i| = 1$)

$$r_D = (4\pi l_B c/A)^{-1/2}(1 + 2Ac_s/c)^{-1/2} \qquad (19)$$

If the polymer concentration c is much lower than the crossover concentration $2Ac_s$, there are many more salt ions than counterions. The salt ions control the screening of the Coulomb interaction and the electrostatic screening length r_D becomes independent of polymer concentration. For higher polymer concentration $c \gg 2Ac_s$, the contribution from the salt ions to the screening of the Coulomb interaction is negligible, and one recovers the salt-free results of section 2 (eq 9a).

3.1. Dilute Solutions. As in the case with salt-free solutions, the Debye expression for the electrostatic screening length (eq 19) can be valid only at low concentrations $c < (A/4\pi l_B)^3/N^2 - 2Ac_s$ (see Appendix B for details) and for high salt concentrations the Debye expression is never valid. Here we focus on the most experimentally relevant case ($c_{int} < c^*$) where for higher ion concentrations the electrostatic screening length is larger than the Debye length. There is a regime with electrostatic screening length shorter than the distance between chains $r_{scr} < R_{cm} \approx (N/c)^{1/3}$ but larger than the chain size.

$$r_{scr} \approx (N/c)^{1/3}(1 + 2Ac_s/c)^{-1/3}$$
$$(A/4\pi l_B)^3/N^2 < c + 2Ac_s < (B/b)^3/N^2 \qquad (20)$$

In this regime the polyelectrolyte is in its extended conformation, with size L given by eq 7. The point where $r_{scr} \approx L$ determines the concentration c_f where the chain becomes flexible.

$$c_f + 2Ac_s \approx N^{-2}b^{-3}B^3 \qquad (21)$$

At higher polymer concentrations ($c > c_f$) the electrostatic screening length is proportional to but larger than the Debye screening length (eq 19)

$$r_B = (B/cb)^{1/2}(1 + 2Ac_s/c)^{-1/2} \qquad c > c_f \qquad (22)$$

For large enough salt concentrations $c_s > N^{-2}(B/b)^3/(2A)$ the chain is flexible for all polyelectrolyte concentrations and the screening length is given by eq 22.

When the electrostatic screening length r_B is smaller than the chain size R ($c_f < c < c^*$), the macromolecules consist of electrostatic screening blobs inside which the conformation is extended. At larger length scales ($r > r_B$), the electrostatic screening blobs repel each other and the interaction between them is analogous to the excluded volume one (regardless of the solvent type). The end-to-end distance can be calculated by analogy with the neutral chain in a good solvent, and the chain is a self-avoiding walk of electrostatic screening blobs

$$R \approx r_B(N/g_B)^{3/5} \approx r_B^{2/5}L^{3/5} \qquad r_B < L \qquad (23)$$

where g_B is the number of monomers in an electrostatic screening blob. The second result in eq 23 was obtained by using the fact that the contour length L of the chain of electrostatic blobs is unchanged and the number of sections of size r_B is $N/g_B = L/r_B$. Substituting eqs 8 and 22 into eq 23, we derive the following expression for the end-to-end distance of a dilute polyelectrolyte chain, when it is flexible

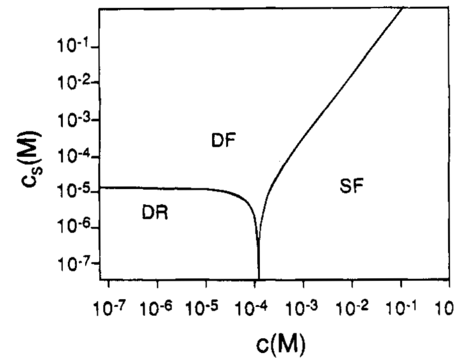

Figure 4. Phase diagram for aqueous polyelectrolyte solutions with $N = 3350$, $A = 5$, and $B = 3$. DR is the dilute rodlike regime, DF is the dilute regime of flexible polyelectrolytes, and SF is the semidilute regime.

$$R \approx bN^{3/5}(cb^3)^{-1/5}B^{-2/5}(1 + 2Ac_s/c)^{-1/5} \qquad c_f < c < c^* \qquad (24)$$

It is important to note that while the regime $c_f < c < c^*$ is quite small when the salt concentration is low (see Figure 4), its extent grows rapidly as salt is added. For $c_s > N^{-2}(B/b)^3/(2A)$, the chain is always flexible in dilute solution and eq 24 holds for all $c < c^*$. The dependence of the end-to-end distance on the degree of polymerization N is the same as in the case of neutral polymers in a good solvent $R \sim N^{3/5}$. The new effect is the concentration dependence of the end-to-end distance in the low-salt regime ($c \gg 2Ac_s$) $R \sim c^{-1/5}$.

The overlap concentration c^* is determined as the concentration where the monomer density inside the coil is equal to the overall monomer density in the solution ($c^* \approx N/R^3$).

$$c^*(1 + 2Ac_s/c^*)^{-3/2} \approx N^{-2}(B/b)^3 \qquad (25)$$

In the low-salt limit ($c \gg 2Ac_s$) we recover the rodlike polyelectrolyte overlap concentration (eq 11), while in the high-salt limit ($c \ll 2Ac_s$) eq 25 leads to an overlap concentration $c^* \approx (B/b)^{6/5}(2Ac_s)^{3/5}N^{-4/5}$ with the same scaling with degree of polymerization as the one for neutral chains in good solvent.

3.2. Semidilute Solutions. The scaling assumption for the correlation length in semidilute solution ($c > c^*$) for general salt concentration is more complicated than the usual one because of the form of eq 25 for overlap concentration and the fact that the dilute solution coil size is now concentration dependent (eq 24). The general scaling assumption is that $\xi \approx R(c)[f(c)/f(c^*)]^{-m}$, where we must choose $f(c)$ and m such that ξ is independent of N. Since the dilute coil size $R(c)$ is a power law in N (see eq 24), $f(c)$ must be chosen to be a power law in N as well. Such a function is given by eq 25, and we choose $f(c) = c(1 + 2Ac_s/c)^{-3/2}$

$$\xi \approx R(c)[(c(1 + 2Ac_s/c)^{-3/2})/(c^*(1 + 2Ac_s/c^*)^{-3/2})]^{-m} \qquad (26)$$

where $R(c)$ is given by eq 24. The exponent m is determined from the condition that the correlation length does not depend on N and we find the exponent $m = {}^3/_{10}$ and the screening length

$$\xi \approx b(cb^3)^{-1/2}B^{1/2}(1 + 2Ac_s/c)^{1/4} \qquad (27)$$

The concentration dependence of the correlation length ξ in the high-salt solution ($c \ll 2Ac_s$) is similar to that of uncharged polymers $\xi \sim c^{-3/4}$, because salt ions strongly screen the Coulomb interaction between charged monomers. In the low-salt case ($c \gg 2Ac_s$) we recover the polyelectrolyte behavior of eq 15, $\xi \sim c^{-1/2}$. The semidilute polyelectrolyte is a random walk of N/g correlation blobs that are space-filling ($c \approx g/\xi^3$)

$$R \approx \xi(N/g)^{1/2} \approx (N/c\xi)^{1/2} \approx bN^{1/2}(cb^3)^{-1/4}B^{-1/4}(1 + 2Ac_s/c)^{-1/8} \quad (28)$$

This chain size R decreases with increasing polymer concentration as $R \sim c^{-1/4}$ in the low-salt solution ($c \gg 2Ac_s$) and as $R \sim c^{-1/8}$ in the high-salt solution ($c \ll 2Ac_s$). As the polymer concentration increases even further, such that $c > c_D$ with

$$c_D + 2Ac_s \approx b^{-3}\begin{cases} 1 & T \ll \Theta \\ B^{-1} & T = \Theta \\ B^{-2} & T \gg \Theta \end{cases} \quad (29)$$

the electrostatic screening length r_B becomes smaller than the electrostatic blob size D. In this regime the concept of electrostatic blob cannot be used.

Figure 4 shows a phase diagram for polyelectrolyte solutions as a function of polymer and salt concentrations, using the sodium salt of fully sulfonated polystyrene with molar mass = 690 000 in water as an example (parameters $N = 3350$, $A = 5$, $u = 2$, and $B = 3$ are determined in section 6). All the regimes of this phase diagram have been discussed above, and therefore we describe them very briefly:

DR: The solution is dilute ($R_{cm} > R$) and the polymer conformation is extended ($R = L < r_{scr}$) (see eq 7). The rodlike polymers in dilute solution interact as a gas of hard spheres of size r_{scr}, because $R_{cm} > r_{scr}$.

DF: The polyelectrolyte chains become flexible ($R > r_B$) and are self-avoiding walks on length scales larger than the electrostatic screening length r_B (dilute regime of flexible chains). Macromolecules still do not overlap ($R_{cm} > R$).

SF: The chains overlap to form a semidilute solution of flexible chains ($R > r_B$). The low polymer concentration boundary of this regime is given by eq 25 ($R_{cm} \sim R$) and increases with salt concentration because the chains become less extended.

4. Osmotic Pressure and Scattering of Semidilute Polyelectrolyte Solutions

In this section we review the results required to understand the osmotic pressure of polyelectrolyte solutions. The osmotic pressure of a solution of neutral polymers is essentially the thermal energy kT per correlation volume in semidilute solution[39]

$$\Pi_p/kT \approx 1/\xi^3 \qquad c > c^* \quad (30)$$

Polyelectrolyte solutions have an additional contribution to their osmotic pressure because of ions Π_i, such that the total osmotic pressure is $\Pi = \Pi_p + \Pi_i$. Although the membrane separating polyelectrolyte solution from pure solvent (across which Π is measured) allows ions to pass through it, Donnan equilibrium[42] requires charge neutrality on both sides of the membrane. For polyelectrolyte solutions with many more counterions than salt ions ($c \gg 2Ac_s$) the ion contribution is kT per counterion

$$\Pi_i/kT \approx c/A \qquad c \gg 2Ac_s \quad (31)$$

In the opposite limit, where salt concentration is high, the counterions are almost uniformly distributed on both sides of the membrane. The salt redistributes to maintain charge neutrality, and this redistribution gives a contribution to osmotic pressure. The resulting expression has been derived in the literature[42] by equating chemical potentials of each ion type on the two sides of the membrane.

$$\Pi_i/kT \approx c^2/4A^2c_s \qquad c \ll 2Ac_s \quad (32)$$

The simplest expression extrapolating between these two limiting behaviors (eqs 31 and 32) is

$$\Pi_i/kT \approx c^2/(4A^2c_s + Ac) \quad (33)$$

The total osmotic pressure is the sum of the ionic and polymeric contributions

$$\Pi/kT \approx c^2/(4A^2c_s + Ac) + 1/\xi^3 \qquad c > c^* \quad (34)$$

At low salt concentrations, the ionic contribution (c/A) dominates over the semidilute polymer contribution ($1/\xi^3 \approx (cb/B)^{3/2}$; see eq 15) for concentrations $c < B^3/A^2b^3$, which is of the order of the bulk concentration in poor and Θ-solvents, but could be lower for weakly charged polyelectrolytes in good solvent. Therefore, eq 31 should apply over a very wide concentration range for osmotic pressure of polyelectrolyte solutions with very low salt concentrations.

At high salt concentrations, both the ionic contribution to osmotic pressure ($c^2/(4A^2c_s)$) and the polymer contribution ($1/\xi^3 \approx (b/B)^{3/2}(2Ac_s)^{-3/4}c^{9/4}$; see eq 27) are much smaller than in low-salt solutions. The ionic contribution dominates for concentrations $c < B^6/(b^6(2A)^5c_s)$. For the vast majority of systems studied to date (see section 6), the ionic contribution dominates the osmotic pressure of polyelectrolytes at high salt concentrations as well as low salt. Therefore, eq 33 should always apply for the osmotic pressure of polyelectrolyte solutions, and the polymer part makes a negligible contribution. This point is well appreciated in the older literature[9,13,14,17,42] but seems to have been missed recently.[3,5,16,43] The Odijk[16] prediction of $\Pi \sim c^{9/8}$ has been refuted by a recent computer simulation.[44]

The large osmotic pressure of salt-free polyelectrolytes has important consequences on the scattering function $S(q)$. Osmotic compressibility is related to the scattering at zero wavelength[39]

$$S(0) \approx kT\,\partial c/\partial \Pi \quad (35)$$

Therefore in the low-salt regime

$$S(0) \approx A \quad (36)$$

The counterion pressure causes $S(0)$ to be much smaller than $S(2\pi\xi^{-1}) \approx g$, the number of monomers inside the correlation blob. The fluctuations of polymer density on length scales larger than the electrostatic screening length lead to a fluctuation of counterion density, governed by the condition of local electroneutrality of a polyelectrolyte solution. However, these fluctuations are g/A times larger than the thermal fluctuations of counterion density and would result in a prohibitively large loss of counterion entropy. So, the extremely high counterion pressure suppresses density fluctuations on length scales larger than the concentration blob size ξ. For $q > 2\pi\xi^{-1}$ the scattering function $S(q)$ decreases with q as it does for uncharged polymers. This suggests that there is a maximum of the scattering function of salt-free semidilute solutions of polyelectrolytes at wave vector q of the order of $2\pi\xi^{-1}$.

One should note that the maximum of the scattering function $S(q)$ disappears at high salt concentrations. When the salt concentration c_s becomes of the order of cg/A^2, the polymer density fluctuations on length scales larger than the concentration blob size ξ are no longer suppressed ($S(0) \approx S(1/\xi) \approx g$). For $c_s > cg/A^2$ the scattering of polyelectrolyte solutions is always a decreasing function of q, as it is for semidilute solutions of neutral chains.

We would like to stress that the peak in the scattering function is caused by the suppression of density fluctuations[14,15] by free ions rather than enhancement caused by microphase separation.[40,41]

5. Dynamics of Polyelectrolyte Solutions

5.1. Dilute Solution ($c \ll c^*$). In dilute polyelectrolyte solutions there are several possible regimes of viscosity behavior. At very low polymer concentration $c < c_{\text{int}}$ the chains are strongly interacting. The Coulomb interaction of neighboring chains couples their motion and dominates the rheology of polyelectrolyte solutions. The viscosity in this strongly interacting regime has been discussed recently by Rabin et al.[45,46] In the concentration range $c_{\text{int}} < c < c_f$ (regime DR in Figure 4) the screening length is larger than the chain size but smaller than the distance between chains. As the polymer moves, it drags the clouds of screening charges and solvent inside its screening volume r_{scr}^3, and the screening length controls hydrodynamics, i.e., the well-known electroviscous effect.[47]

In the concentration interval $c_f < c < c^*$ (regime DF in Figure 4) the polymer coils still do not overlap but they are larger than the screening length. The polymer dynamics in this regime can be described by the Zimm model.[48] The longest relaxation time in dilute solution is proportional to the hydrodynamic volume of the chain R^3.

$$\tau_{\text{Zimm}} \approx \eta_s R^3/kT \qquad c_f < c < c^* \tag{37}$$

The modulus G (at relaxation time τ_{Zimm}) in this regime is kT per chain

$$G \approx ckT/N \qquad c_f < c < c^* \tag{38}$$

The reduced viscosity of the dilute polyelectrolyte solution is

$$(\eta - \eta_s)/\eta_s c \approx G\tau_{\text{Zimm}}/\eta_s c \approx R^3/N \approx b^3 N^{4/5}(cb^3)^{-3/5}B^{-6/5}(1 + 2Ac_s/c)^{-3/5} \qquad c_f < c < c^* \tag{39}$$

The high-salt limit of eq 39 gives the intrinsic viscosity $[\eta]$ of a polyelectrolyte (with $c \ll 2Ac_s$)

$$[\eta] = \lim_{c \to 0} (\eta - \eta_s)/(\eta_s c) \approx (b/B)^{6/5}N^{4/5}(2Ac_s)^{-3/5} \tag{40}$$

The diffusion coefficient can be determined from the relaxation time, because chains diffuse a distance of order of their size during their relaxation time

$$D_{\text{self}} \approx R^2/\tau_{\text{Zimm}} \approx kT/(\eta_s R) \approx (kT/\eta_s b)N^{-3/5}(cb^3)^{1/5}B^{2/5}(1 + 2Ac_s/c)^{1/5} \qquad c_f < c < c^* \tag{41}$$

Notice that due to strong hydrodynamic interactions, dilute flexible polyelectrolytes diffuse as spheres of size R (Stokes' law). The high-salt limit of eq 41 gives the limiting diffusion coefficient in dilute solution D_0 (with $c \ll 2Ac_s$)

$$D_0 = \lim_{c \to 0} D_{\text{self}} \approx (kT/\eta_s)N^{-3/5}(B/b)^{2/5}(2Ac_s)^{1/5} \tag{42}$$

Equations 40 and 42 each have the same dependence on chain length as uncharged polymers in good solvent because of the self-avoiding walk configuration of polyelectrolytes in the dilute flexible regime of concentration.

5.2. Semidilute–Unentangled Regime ($c^* < c < c_e$). When polymer chains overlap, the hydrodynamic interaction gets screened on length scales larger than the correlation length ξ. Inside the correlation blob, the motion of different sections of the chain are strongly hydrodynamically coupled just as in dilute solution. The relaxation time of the section of g monomers inside the correlation blob is Zimm-like (see eq 37).

$$\tau_\xi \approx \eta_s \xi^3/kT \tag{43}$$

Each chain consists of N/g correlation blobs. The hydrodynamic interaction between these blobs is screened and therefore their motion can be described by the Rouse model.[48]

$$\tau_{\text{Rouse}} \approx \tau_\xi (N/g)^2 \approx (\eta_s b^3/kT)N^2(cb^3)^{-1/2}B^{-3/2}(1 + 2Ac_s/c)^{-3/4} \qquad c^* < c < c_e \tag{44}$$

At low salt concentrations ($2Ac_s < c$) the relaxation time in this semidilute–unentangled regime *decreases with increasing polymer concentration* as $\tau_{\text{Rouse}} \sim c^{-1/2}$. This leads to the self-diffusion coefficient

$$D_{\text{self}} \approx R^2/\tau_{\text{Rouse}} \approx (kT/\eta_s b)N^{-1}B(1 + 2Ac_s/c)^{1/2} \qquad c^* < c < c_e \tag{45}$$

which is *concentration independent* in low-salt solutions: $D_{\text{self}} \sim c^0 N^{-1}$ (for $2Ac_s \ll c$). The modulus of the Rouse model for unentangled polymer solutions is still given by kT per chain (eq 38). The viscosity of the polyelectrolyte solution in this regime is

$$\eta \approx \tau_{\text{Rouse}} G \approx \eta_s N(cb^3)^{1/2}B^{-3/2}(1 + 2Ac_s/c)^{-3/4} \qquad c^* < c < c_e \tag{46}$$

In the low-salt limit $c \gg 2Ac_s$, the viscosity grows as the square root of concentration $\eta \sim c^{1/2}$ (Fuoss law). In the high-salt regime $c \ll 2Ac_s$, $\eta \sim c^{5/4}$, which is the same scaling as semidilute unentangled neutral polymers in good solvent.[49]

5.3. Entanglement Criterion. The unentangled–semidilute regime is well documented[49,50] for neutral polymers, where the typical range is $5 \le c_e/c^* \le 10$. The physical reason for this regime is that significant overlap of chains is required for them to begin topologically constraining each other's motion, resulting in a tube diameter larger than the correlation length. It was phenomenologically found that at the entanglement onset of uncharged chains, each chain has to overlap with n others,[51,52] with $5 \le n \le 10$ being dependent on polymer species. The monomer concentration required for entanglement is $c_e = nN/R^3$. With no added salt ($c \gg 2Ac_s$)

$$c_e = nN/R^3 = (nN/L^3)(c_e/c^*)^{3/4} = n^4c^* \qquad (47)$$

where we have used eqs 11 and 17. For general salt concentration the requirement $c_e = nN/R^3$ leads to

$$(c_e/c^*)^{1/4}((1 + 2Ac_s/c^*)/(1 + 2Ac_s/c_e))^{3/8} \approx n \qquad (48)$$

Combining with eq 25 yields

$$c_e/(1 + 2Ac_s/c_e)^{3/2} \approx n^4N^{-2}b^{-3}B^3 \qquad (49)$$

which is identical to the equation for the overlap concentration c^* (eq 25) except for a prefactor $n^4 \approx 10^3$–10^4. If the relative salt concentration is low, the unentangled–semidilute regime of polyelectrolytes should be three to four decades wide ($10^3 \le c_e/c^* \le 10^4$). The viscosity at the entanglement concentration c_e is $\eta_e \approx n^2\eta_s \approx 50\eta_s$, as it is in neutral polymers. For low salt the semidilute–unentangled regime is very wide because of the strong concentration dependence of the chain size ($R \sim c^{-1/4}$). This is only slightly weaker than the concentration dependence of the distance between the centers of mass of neighboring chains ($R_{cm} \sim c^{-1/3}$). Therefore the number of chains overlapping with a given one has very weak concentration dependence $(R/R_{cm})^3 \sim (c/c^*)^{1/4}$. If the concentration of salt is high the range of the unentangled semidilute regime is comparable to that for neutral polymer in good solvent $c_e \approx n^{8/5}c^* \approx 10c^*$.

5.4. Semidilute–Entangled Regime ($c > c_e$). Entanglements are characterized by a tube diameter[48] $\mathbf{a}$ (the mesh size of the temporary entanglement network). The entanglement strand is a random walk of $N_e/g \approx (\mathbf{a}/\xi)^2$ blobs, where N_e is the number of monomers in an entanglement strand. As discussed in the previous section, there are n such strands in the volume $\mathbf{a}^3$, so $(\mathbf{a}/\xi)^3 \approx nN_e/g$ and we see that $n = \mathbf{a}/\xi$. Thus the tube diameter is proportional to the screening length. Reptation theory can be used to calculate the longest relaxation time, assuming relaxation is Zimm-like inside the correlation blobs and relaxation of strands of blobs between the entanglements is Rouse-like[48]

$$\tau_{rep} \approx \tau_\xi(N_e/g)^2(N/N_e)^3 \approx (\eta_s b^3/kT)n^{-2}N^3B^{-3}(1 + 2Ac_s/c)^{-3/2} \qquad (50)$$

Note that at low salt concentration $2Ac_s \ll c$ the disentanglement time is *concentration independent*.

The plateau modulus in this regime is $G \approx \nu_e kT$, where ν_e is the number density of entanglement strands. The volume of an entanglement strand is $\xi^3N_e/g = \xi\mathbf{a}^2$. The modulus is[49,53]

$$G \approx kT/(\mathbf{a}^2\xi) \approx kTb^{-3}n^{-2}(cb^3)^{3/2}B^{-3/2}(1 + 2Ac_s/c)^{-3/4} \qquad (51)$$

and the viscosity is

$$\eta \approx G\tau_{rep} \approx \eta_s n^2(N/N_e)^3 \approx \eta_s n^{-4}N^3(cb^3)^{3/2}B^{-9/2}(1 + 2Ac_s/c)^{-9/4} \qquad (52)$$

In the low-salt limit $c \gg 2Ac_s$, the viscosity has a stronger than linear concentration dependence $\eta \sim c^{3/2}$. In the high-salt regime ($c \ll 2Ac_s$), $\eta \sim c^{15/4}$ as it does for neutral polymer solutions in good solvent.[39]

The viscosity of polyelectrolyte solutions (eq 52) crosses over, at polymer concentration c_D (eq 29), to the viscosity of uncharged polymers in good or Θ solvents. In poor solvents for the uncharged backbone we expect a viscosity discontinuity near c_D because of an abrupt change in chain statistics.

The diffusion coefficient in the entangled regime is

$$D_{self} \approx R^2/\tau_{rep} \approx (kT/\eta_s b)n^2N^{-2}(cb^3)^{-1/2}B^{5/2}(1 + 2Ac_s/c)^{5/4} \qquad (53)$$

In the low-salt regime ($c \gg 2Ac_s$), $D_{self} \sim c^{-1/2}$, while in the high-salt regime ($c \ll 2Ac_s$), $D_{self} \sim c_s^{5/4}c^{-7/4}$.

6. Comparison with Experiments

By far the most studied polyelectrolyte is monodisperse poly(styrenesulfonate) with sodium counterions (NaPSS) in aqueous solution. This polymer has one charged group per monomer, with a monomer length $b \approx 3$ Å. In aqueous solution, the Bjerrum length is $l_B \approx 7$ Å, and thus the parameter $u = l_B/b \approx 2$. Naively one might expect the number of monomers between charges, $A = 1$, since each monomer has a potentially charged group. However, because $u > 1$, we expect counterion condensation[2,35,36] to make $A > 1$.

We evaluate the parameter A from the collection of literature data on osmotic pressure of salt-free NaPSS[43] (see Figure 6 of ref 43). As pointed out by Cohen et al.[46] aqueous solutions with no added salt exposed to air have an effective salt concentration $c_s \approx 4 \times 10^{-6}$ M because of dissolved (and dissociated) carbon dioxide. For polymer concentrations $3 \times 10^{-4} < c < 10^{-1}$ M (moles of monomer per liter), the osmotic pressure is independent of chain length and obeys a power law in concentration: $\Pi \sim c^{1.1\pm0.1}$, in excellent agreement with the prediction of eq 31. From those data we determine the parameter $A \approx 5$. Polystyrene in water has $T \ll \Theta$ ($\tau \cong 1$), so the distance between charges $bA^{1/3} \approx 5$ Å, which is essentially the same as the Bjerrum length (7 Å). The electrostatic blob size is $D \approx b(A^2/u)^{1/3} \approx 7$ Å (eq 6) and the number of effective charges in an electrostatic blob is $g_e/A \approx A/u \approx 2$ (eq 4).

We test the scaling prediction for osmotic pressure (eq 33) in Figure 5 using the semidilute NaPSS data of Koene et al.[54] at various salt concentrations and the salt-free data of Takahashi et al.[55] While ref 55 did not report the salt concentrations of their "salt-free" data, those data clearly indicate a low level of salt (see Figure 1 of ref 55) and we estimate $c_s \approx 3 \times 10^{-5}$ M from their data. Data at high salt concentrations from ref 55 were not used in Figure 5, because they correspond to dilute solution where changes in electrostatic screening may affect osmotic pressure. The solid curve is the prediction of eq 33 with $A = 5$. Clearly the agreement between theory and experiment is superb, and we conclude that $A \approx 5$ for fully sulfonated polystyrene in water, over a wide range of salt concentrations.

Scattering experiments in the semidilute–unentangled regime[10,11] find a maximum in scattering intensity as a function of wave vector, as predicted by the scaling model. Drifford and Dalbiez[11] have shown that the wave vector of maximum scattering (q_{max}) scales as the correlation length (eq 15), $\xi \sim c^{-1/2}$. Light scattering[11] and neutron scattering[10] data were combined to cover

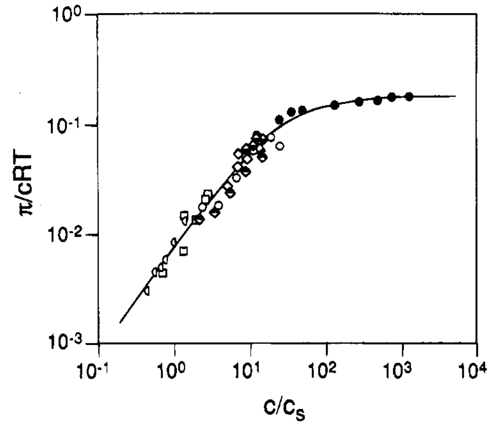

Figure 5. Osmotic pressure of semidilute NaPSS as functions of polymer and salt concentration. Filled circles are data of Takahashi et al.[55] for $M_w = 4.3 \times 10^5$ with no added salt and apparent $c_s \approx 3 \times 10^{-5}$ M. Other symbols are data of Koene et al.[54] for molecular weight $M_w = 6.5 \times 10^5$ and salt concentrations $c_s = 5 \times 10^{-3}$ M (open circles), $c_s = 5 \times 10^{-2}$ M (open squares), $c_s = 1 \times 10^{-2}$ M (open diamonds), and $c_s = 1 \times 10^{-1}$ M (open half-moons); for $M_w = 4 \times 10^5$ and $c_s = 1 \times 10^{-2}$ M (bottom-filled diamonds); and for $M_w = 12 \times 10^5$ and $c_s = 1 \times 10^{-2}$ M (top-filled diamonds). The solid curve is the prediction of eq 33 with $A = 5$.

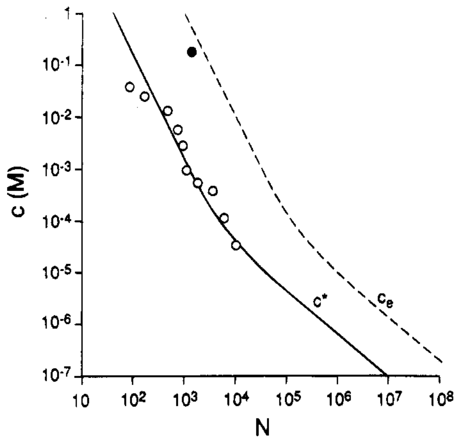

Figure 6. Phase diagram for NaPSS with no added salt. Open circles are experimental concentrations c^* where $\eta = 2\eta_s$ from refs 46, 57, 58, and 59. The solid curve is the overlap concentration c^* from eq 25. The dashed curve is the entanglement concentration c_e from eq 49 with $n = 5$, $A = 5$, $B = 2.8$, and $c_s = 4 \times 10^{-6}$ M. The solid point is the entanglement concentration from the data of ref 59 (see Figure 7).

4 orders of magnitude in concentration: $5 \times 10^{-5} < c < 5 \times 10^{-1}$ M. These data are fit very well by eq 27 with $A = 5$, $B = 2$, and $c_s = 4 \times 10^{-6}$ M assuming $q_{\max} = 2\pi\xi^{-1}$. This value of B compares reasonably with the $T \ll \Theta$ case of eq 8, which expects $B \approx 5$. The chain size[56] of NaPSS with no added salt has been found to scale as $R \sim c^{-1/4}$ in semidilute solutions, consistent with the low-salt limit of eq 28.

We determine the overlap concentration experimentally as the concentration at which the viscosity is twice the solvent viscosity. This has been done for fully sulfonated NaPSS for ten molecular weights $1.6 \times 10^4 < M_w < 2 \times 10^6$, and the results are plotted in Figure 6. For five of the six highest molecular weights,[46,57,58] c^* was determined by interpolation of viscosity data. One sample[59] had c^* determined by extrapolation of viscosity data above c^*. For the five lowest molecular weights,[46] c^* was determined by extrapolation of viscosity data for concentrations below c^*. Our estimate of c^* is particularly crude for the two lowest molecular weights, as the extrapolation was roughly a factor of 10 in concentration. These data were used as a second determination of the parameter B, by fitting to eq 25. The solid curve in Figure 6 is eq 25, with $B = 2.8$, in excellent agreement with $B = 2$ obtained from scattering, particularly because our criterion for overlap in the viscosity data ($\eta = 2\eta_s$) is rather arbitrary. We were only able to determine the entanglement concentration for one sample[59] with $N = 1500$. Viscosity data for this sample with no added salt are plotted in Figure 7. These data clearly show the expected behavior of $\eta \sim c^{1/2}$ below c_e and $\eta \sim c^{3/2}$ above c_e. The entanglement concentration, determined as the intersection of the two power laws, is plotted as the solid point in Figure 6. The viscosity at the entanglement onset $\eta_e \approx 20\eta_s$, indicating roughly 5 chains required for entanglement, and the dashed curve in Figure 7 is the entanglement concentration of eq 49 with $n = 5$, $A = 5$, $B = 2.8$, and $c_s = 4 \times 10^{-6}$ M. There are three regimes in this phase diagram. Below c^* the chains do not overlap. The range of concentration $c^* < c < c_e$ is the semidilute–unentangled regime, and spans three decades for $N = 10^3$. Above c_e entanglements are expected to be important for dynamics. Both c^* and c_e curves cross over from low-salt to high-salt behaviors at $c = 2Ac_s = 4 \times 10^{-5}$ M. Figures 6 and 7 show that the data of ref 59 exhibit nearly quantitative agreement with our scaling theory.

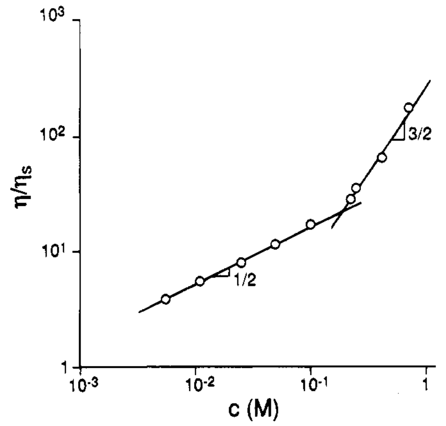

Figure 7. Concentration dependence of relative viscosity for NaPSS with $N = 1500$ and no added salt. Data of Fernandez Prini and Lagos.[59] Solid lines are power laws of eqs 46 and 52 (with $c \gg 2Ac_s$).

Both viscosity and scattering data prove that the overlap concentration of high molecular weight polyelectrolytes without added salt is extremely low, as expected by our model (see Figure 6). High-frequency viscoelastic measurements[60] on a different monodisperse polyelectrolyte system indicate good agreement with the Rouse model for high molecular weight polymers at a concentration of 0.02 M. This is strong evidence for a broad range of concentrations that are semidilute but unentangled, as expected by our model (see Figure 6).

Another very strong evidence of this regime is the reported self-diffusion coefficient of a series of NaPSS with molecular weights in the range (16 000 < M < 354 000) in salt-free water solution measured by pulsed field gradient NMR.[61,62] In the semidilute regime (with viscosity significantly above the solvent viscosity) a wide range of polymer concentration is found (up to 0.1 M) with concentration-independent self-diffusion coefficient. This observation confirms our prediction of a wide concentration range of unentangled–semidilute regime. The measured molecular weight dependence of the self-diffusion coefficient[61] $D \sim M^{-1.0\pm0.05}$ is in excellent

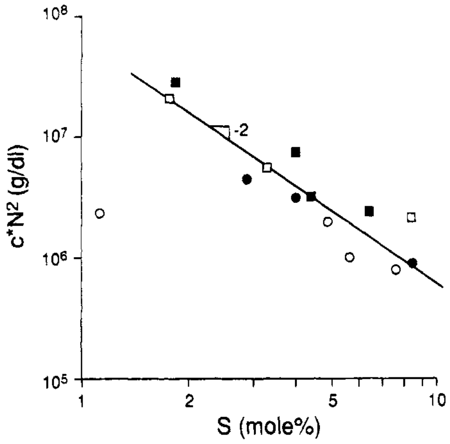

Figure 8. Dependence of the overlap concentration c^* on degree of polymerization N and sulfonation level S for lightly sulfonated polystyrene in DMF with no added salt. The line of slope -2 was drawn from the expectation that $c^*N^2 \sim B^3 \sim A^2 \sim S^{-2}$ (see the $T = \Theta$ case, eq 8). c^* was evaluated as the concentration where $\eta = 2\eta_s$ from the data of Kim and Peiffer[63] at $M = 1.15 \times 10^5$ (open circles), $M = 6 \times 10^5$ (filled circles), $M = 9 \times 10^5$ (open squares), and $M = 18 \times 10^5$ (filled squares).

agreement with our prediction of the Rouse-like motion in this regime (see eq 45 for $2Ac_s \ll c$).

Kim and Peiffer[63] reported viscosity data in DMF for four chain lengths of polystyrene that have been sulfonated at a variety of low levels (1.1–8.4% of the monomers sulfonated, so that $12 < A < 91$). The solvent dielectric constant $\epsilon = 36.6$ and thus the Bjerrum length $l_B = 15$ Å in DMF at room temperature. Because the sulfonation level is low enough ($A > 12$), we do not expect any counterion condensation in these samples (the distance between charges should always be larger than l_B). Thus these lightly sulfonated polystyrenes provide the opportunity to vary A (and indirectly B) systematically. Nonsulfonated polystyrene is soluble in DMF, with intrinsic viscosity $[\eta] \sim M^{0.60}$ at 35 °C.[64] Thus DMF at 35 °C is much closer to a Θ condition ($[\eta] \sim M^{1/2}$) than a good solvent condition ($[\eta] \sim M^{4/5}$) for polystyrene. Kim and Peiffer report viscosity both above and below c^* for most of their samples, and thus c^* was determined as the concentration at which $\eta = 2\eta_s$ by interpolation in most cases and by only slight extrapolation in the other cases. Figure 8 shows the scaling of the overlap concentration with sulfonation level and chain length, in the form suggested by the low c_s limit of eq 25 (c^*N^2 vs sulfonation level S). The solid line has a slope of -2, expected from eqs 11 and 8 assuming DMF is nearly a Θ solvent for nonsulfonated polystyrene ($c^*N^2 \sim B^3 \sim A^2 \sim S^{-2}$). Clearly, the data are in reasonable agreement with the prediction.

The only systematic study of entanglement effects on polyelectrolyte viscosity is the work of Yamaguchi et al.[65] They studied narrow molecular weight distribution poly(*N*-methyl-2-vinylpyridinium chloride) in water up to 0.2 g/mL and obtained a large collection of data in the semidilute–entangled regime (with $\eta > 10^2\eta_s$). With no added salt they found $\eta \sim c^{1.5}$, in perfect agreement with the $c_s = 0$ limit of eq 52. As salt was added, they found the apparent exponent α ($\eta \sim c^{\alpha}$) increased ($\alpha = 1.8$ for $c_s = 0.01$ M; $\alpha = 2.8$ for $c_s = 0.1$ M; $\alpha = 4.6$ for $c_s = 0.5$ M). The highest salt concentration is in reasonable agreement with the high-salt limit of eq 52, and the other two are consistent with the crossover expected between the exponents $^3/_2$ and $^{15}/_4$ at intermediate salt concentrations. They find that the plateau modulus G and the recoverable compliance J_e in salt-free solutions $G \sim 1/J_e \sim c^{1.3}$, in qualitative agreement with our prediction for the low-salt limit of the semidilute–entangled regime (eq 51 predicts $G \sim c^{3/2}$). They also reported a very weak concentration dependence of relaxation time $\tau_{\rm rep} \sim c^{0.2}$, in qualitative agreement with the low-salt behavior of eq 50 ($\tau_{\rm rep} \sim c^0$). Another interesting result of Noda et al.[66] is a crossover in viscosity, modulus, and recoverable compliance at polymer concentration $c \approx 0.3$ g/cm³ to a behavior analogous to that of uncharged polymers. We conclude that the predictions of our theory agree with available data for viscosity of entangled polyelectrolytes, but a systematic study covering a wide range of concentrations for both viscosity and osmotic pressure is required for more quantitative testing of our theory.

7. Conclusion

We have presented a scaling theory of flexible polyelectrolyte solutions, incorporating effects of counterion condensation, polyelectrolyte chain length and concentration, and added salt. The salt-free results were published in a recent letter.[67]

The static picture for the configuration of a polyelectrolyte chain with no added salt is identical to the 1976 scaling model of de Gennes et al.[14] We have extended this picture to solutions of arbitrary salt concentration, and the high-salt limit scaling agrees with the model of Pfeuty.[15] As pointed out in ref 14, the Rouse model applied to the salt-free configuration of a semidilute solution accounts for the empirical Fuoss law. In 1976 the belief was that the overlap concentration and the entanglement concentration were identical. It is now known that uncharged polymer solutions have a Rouse regime that is semidilute but not entangled.[49,50] We have merely used the same notions about entanglement for uncharged polymers to develop a theory for the full concentration dependence of viscosity, relaxation time, and diffusion coefficient.

In salt-free unentangled–semidilute solutions viscosity is predicted to obey the Fuoss law ($\eta \sim c^{1/2}$) and the diffusion coefficient is predicted to be independent of concentration. Since the criteria used for the overlap concentration and the entanglement concentration suggest that these occur at specific values of the relative viscosity ($\eta = 2\eta_s$ for c^* and $\eta \cong 50\eta_s$ for c_e) and the viscosity scales as the square root of concentration between c^* and c_e, there is a *surprisingly wide regime of semidilute–unentangled behavior* ($c_e \cong 10^3c^*$). Above c_e in salt-free solutions, we make a new prediction for the entangled viscosity ($\eta \sim c^{3/2}$) that is in excellent agreement with data on sulfonated polystyrene[59] and poly(*N*-methyl-2-vinylpyridinium chloride).[65]

Using osmotic pressure data on fully sulfonated polystyrene, we were able to evaluate the number of monomers between effective charges $A = 5$, which is larger than unity due to counterion condensation. Using this parameter, we are able to predict the length scale of the peak in the scattering function within a factor of 1.5. The overlap concentration from viscosity data is also quantitatively predicted from $A = 5$.

Given an independent measure of effective charge on the chain (such as osmotic pressure), our model can predict dynamic properties of semidilute polyelectrolyte solutions. Since the theory is based on scaling, we do not know prefactors a priori, but data on NaPSS indicate that all prefactors are of order unity once the effective charge is known. Thus the scaling theory can semiquantitatively predict viscosity and diffusion coefficient in both entangled and unentangled semidilute solutions where the Fuoss law is observed. This empirical law has recently been used to correlate the shear rate dependent viscosity of polyelectrolytes.[68] A further test of our model could be made from such data, as eq 44 should predict the relaxation times required for such a correction. While there is a great deal of viscosity data in the literature for polyelectrolytes, there is a real need for a single study that covers the full concentration range for high molecular weight polyelectrolytes, measuring viscosity and osmotic pressure. We hope that the ideas presented here will motivate such a study.

Acknowledgment. The authors benefited greatly from discussions with J. F. Joanny. We acknowledge the support of the NSF Under Grant DMR-9409787 and the NRC Under Grant CAST-93. We thank J. Cohen for sending tables of viscosity data.

Appendix A. Nomenclature

a	tube diameter
A	number of monomers between uncondensed charges
b	monomer size
B	dimensionless contour length parameter ($B = Nb/L$)
c	monomer concentration (number density)
c^*	monomer concentration above which the chains overlap
c_D	monomer concentration at which the electrostatic screening length equals the electrostatic blob size ($r_B = D$)
c_e	monomer concentration at which chains entangle
c_f	monomer concentration above which chains are flexible
c_{int}	monomer concentration below which chains strongly interact with each other ($r_D = R_{cm}$)
c_{ion}	total free ion concentration (number density)
c_s	salt concentration (number density of each monovalent salt ion)
c_Z	number density of sections of polyelectrolytes with charge Z
D	electrostatic blob size
D_{self}	self-diffusion coefficient
D_0	dilute limit of D_{self} (in high salt)
e	elementary charge
g	number of monomers in a correlation blob
g_B	number of monomers in an electrostatic screening blob
g_e	number of monomers in an electrostatic blob
k	Boltzmann's constant
l_B	Bjerrum length
L	contour length of a chain of electrostatic blobs (also dilute size of a chain in salt-free solutions)
m	exponent for concentration dependence for correlation length
n	number of overlapping strands required for entanglement
N	number of monomers in a chain
N_e	number of monomers in an entanglement strand
N_{ion}	number of ions in screening volume $r_{scr}{}^3$
q	scattering wavevector
r_B	electrostatic screening length for $c > c_f$
r_D	Debye electrostatic screening length
r_{DP}	Debye length due to polyions
r_{scr}	electrostatic screening length
R	chain size (end-to-end distance)
R_{cm}	distance between centers of mass of neighboring chains
S	sulfonation level
$S(q)$	scattering function
T	temperature
u	ratio of Bjerrum length to monomer size ($u = l_B/b$)
Z	valency
γ	surface tension
ϵ	dielectric constant
η	viscosity
η_e	viscosity at entanglement onset c_e
η_s	solvent viscosity
Π	osmotic pressure
Π_p	polymeric contribution to osmotic pressure
Π_i	ionic contribution to osmotic pressure
Θ	theta temperature
ξ	correlation length
τ	reduced temperature ($\tau = (\Theta - T)/\Theta$)
τ_{rep}	reptation time (longest relaxation time in entangled solution)
τ_{Rouse}	Rouse time (longest relaxation time in semidilute unentangled solution)
τ_{Zimm}	Zimm time (longest relaxation time in dilute solution)
τ_ξ	Zimm relaxation time of correlation blob in semidilute solution

Appendix B. Conjectures on Electrostatic Screening

In this appendix we explain the inability of the Debye–Hückel theory to describe the screening of polyelectrolytes by free ions in solution and propose an alternative picture.

Electrostatic screening of polyion charge depends on the relation of the overlap concentration c^* to the interaction concentration c_{int}. In the low-salt limit, eqs 10 and 11 give

$$c^*/c_{int} = (4\pi uB/A)^3 = (4\pi)^3 \begin{cases} \tau^3 Au & T < \Theta \\ u^2/A & T = \Theta \\ u^{15/7}/A^{9/7} & T \gg \Theta \end{cases} \qquad \text{(B.1)}$$

For very poor solvent for the uncharged chain ($T \ll \Theta$ and $\tau \approx 1$) $c^* > c_{int}$, since $A \geq 1$ and $u \geq 1$. In most cases, $c^* > c_{int}$, but it is possible to have $c_{int} > c^*$ (for weakly charged chains with $T > \Theta$), so we consider each case in turn.

Case i. $c^* > c_{int}$ [$B > A/(4\pi u)$]. This is the most common case. For example, NaPSS has $\tau \approx 1$, $A = 5$, and $u = 2$, so $c^* = 2 \times 10^4 c_{int}$.

In the concentration range $c_{int} < c < c^*$ the Debye screening length is shorter than the distance between chains ($r_D < R_{cm}$). In order to screen the electric field of a given chain in a no-salt solution, nearly all counterions must be localized within the Debye radius r_D of this chain. Such a localization of counterions to a part of available space would lead to a prohibitively high entropic penalty (the osmotic pressure is kT per counterion). We therefore conclude that the Debye–Hückel approximation is not valid in this concentration range, because the local charge density fluctuations required to screen the polyion charge would have to be of the order of the average density of the counterions in the system. Below we explain this in more detail.

Consider a probe charge Ze inserted in an electroneutral medium. The specific probes we are concerned with are polyelectrolytes (with $Z = N/A$) or sections of polyelectrolytes. Counterions of both signs contribute to screening of the probe charge. In order to screen this charge, the density of ions of opposite sign near the probe has to increase, while the density of ions of the same sign has to decrease. The ionic cloud has to be able to change its charge within the screening radius r_{scr} by the amount at least equal to the charge of the probe. In the Debye–Hückel model the change of the number of ions ΔN_{ion} within the Debye radius r_D of the probe is of the order of the square root of the total number of ions there $N_{ion} \approx c_{ion} r_D^3$, where c_{ion} is the number density of free ions $c_{ion} = c/A + 2c_s$. Thus this theory can only describe screening of charges up to $Z \approx \Delta N_{ion} \approx N_{ion}^{1/2} \approx c_{ion}^{1/2} r_D^{3/2}$. Screening of larger charges requires modifications of this theory. Below we outline our conjecture that assumes the smallest possible change of the Debye screening picture.

We assume that the Debye radius gives the correct electrostatic screening length as long as the valency of the probe charge Z is smaller than the number of oppositely charged free ions within the Debye volume ($r_{scr} = r_D$ as long as $Z < N_{ion} \approx c_{ion} r_D^3$). Using the polyelectrolyte chain as our probe charge with valency $Z = N/A$, we conclude that the Debye screening length (eq 9) can only be used at ion concentrations lower than $c_{ion} < (A/N)^2 (4\pi l_B)^{-3} = c_{int}/A$.

$$r_{scr} = r_D \qquad \text{for } c + 2Ac_s < c_{int} \qquad (B.2)$$

At higher concentrations there are not enough ions inside the Debye radius to screen the probe; therefore the electrostatic screening length r_{scr} has to be larger than the Debye length $r_{scr} > r_D$. We conjecture that the electrostatic screening length expands until there are enough ions within distance r_{scr} of the probe to screen its field

$$c_{ion} r_{scr}^{\;3} \approx Z \qquad (B.3)$$

It is important to note that this is a minimal conjecture: it is conceivable that the electrostatic screening length expands even more, but it must expand at least to r_{scr} for the concepts of electrostatic screening to apply at all. The new electrostatic screening length is, therefore

$$r_{scr} \approx (Z/c_{ion})^{1/3} = (N/(c + 2Ac_s))^{1/3} \qquad c_{int} < c + 2Ac_s < c_f + 2Ac_s \quad (B.4)$$

This relation is only valid up to a concentration c_f where the chain size L is equal to the electrostatic screening length r_{scr}. At higher concentrations ($c > c_f$) only part of the chain with charge

$$Z \approx (g_e/A)(r_{scr}/D) \qquad (B.5)$$

is inside the electrostatic screening length r_{scr}. Substituting eq B.5 in eq B.3 and using eqs 8, we find the electrostatic screening length $r_B = r_{scr}$ for polyelectrolytes in both dilute ($c_f < c < c^*$) and semidilute ($c > c^*$) solutions.

$$r_{scr} = r_B \approx [B/b(c + 2Ac_s)]^{1/2} \qquad c > c_f \qquad (B.6)$$

This electrostatic screening length (cf. eq 22) is larger than, but proportional to, the Debye length r_D (eq 9).

It is important to note that even in the high-salt limit ($c_s \gg c/2A$) we expect the electrostatic screening length $r_B \approx [B/(2Abc_s)]^{1/2}$ to be larger than Debye length $r_D = (8\pi lBc_s)^{-1/2}$. This does not mean that the Debye–Hückel theory is not valid for screening of small probe charges. The problem is that there are not enough ions inside the Debye volume r_D^3 (even at high salt concentrations) to screen the large charge Z of the section of polyions inside this volume. Thus even in the high-salt regime we expect the screening length to depend on the chain properties (e.g., parameters A and B). The above argument is valid as long as the screening length is larger than the electrostatic blob size.

Case ii. $c^* < c_{int}$ [$B < A/(4\pi u)$]. In this case polyelectrolytes are still strongly interacting at their overlap concentration and participate in the screening process in addition to counterions.[18] We demonstrate below that because of their large charge, polyions are much more effective than counterions in screening electrostatic interactions.

In order to estimate the polyion contribution to electrostatic screening, we subdivide each chain into sections of size r_{DP}. The charges on each such section are strongly interacting and coherently contribute to screening as one big charge Z (see eq B.5)

$$Z \approx (r_{DP}/D)(g_e/A) \qquad (B.7)$$

We assume that different chain sections (of size r_{DP} and charge Z) contribute to screening independently. The concentration of these sections is

$$c_Z \approx c/(AZ) \qquad (B.8)$$

The electrostatic screening length can be estimated from the Debye–Hückel theory (eq 9)

$$r_{DP} = [4\pi l_B (c/A + c_Z Z^2)]^{-1/2} \approx [4\pi l_B c Z/A]^{-1/2} \qquad (B.9)$$

Notice that for $Z \gg 1$ the polyions dominate the screening. The screening length r_{DP} can now be determined self-consistently (by substituting eq B.7 into B.9 and solving for r_{DP})

$$r_{DP} \approx (4\pi l_B c g_e/DA^2)^{-1/3} \approx (4\pi u B c/A^2)^{-1/3} \qquad (B.10)$$

where $u \equiv l_b/b$ and $B = g_e b/D$ (eq 8).

The Debye length due to polyions r_{DP} (eq B.10) is smaller than the correlation length $\xi = (B/bc)^{1/2}$ of the semidilute solution (eq 15) in a wide concentration range

$$c^* < c < (4\pi)^2 B^5 (A^2/u)^{-2} b^{-3} \qquad (B.11)$$

However, $r_{DP} < \xi$ would mean there is less than one polyion section inside a Debye volume $c_Z r_{DP}^3 < 1$, contradicting the mean-field assumption of the Debye–Hückel theory. Thus in the concentration range given by eq B.11 the Debye length r_D due to counterions alone is larger than the correlation length ξ, while the Debye length due to polyions r_{DP} is smaller than ξ.

$$r_{DP} < \xi < r_D \qquad (B.12)$$

Therefore, we conjecture that in this case, when counterion screening alone is weak, but screening due to polyions is very strong, the electrostatic screening length is of the order of the distance between sections of polyions

$$r_B \approx \xi \tag{B.13}$$

At a higher polymer concentration $cb^3 > (4\pi)^2 B^5 (A^2/u)^{-2} b^{-3}$ a liquid crystal ordering of overlapping, strongly interacting rodlike polyelectrolyte sections is possible, but we do not discuss this phase transition here (see ref 69).

References and Notes

(1) Katchalsky, A. *Pure Appl. Chem.* **1971**, *26*, 327.
(2) Oosawa, F. *Polyelectrolytes*; Marcel Dekker: New York, 1971.
(3) Mandel, M. In *Encyclopedia of Polymer Science and Engineering*; Wiley: New York, 1988; Vol. 11, p 739.
(4) Hodgson, D. F.; Amis, E. J. In *Polyelectrolytes*; Hara, M., Ed.; Marcel Dekker: New York, 1993.
(5) Mandel, M. In *Polyelectrolytes*; Hara, M., Ed.; Marcel Dekker: New York, 1993.
(6) Schmitz, K. S. *Macroions in Solution and Colloidal Suspension*; VCH: New York, 1993.
(7) *Macro-ion Characterization*; Schmitz, K. S., Ed.; ACS Symposium Series 548; American Chemical Society: Washington, DC, 1994.
(8) Forster, S.; Schmidt, M. *Adv. Polym. Sci.*, submitted.
(9) Fuoss, R. M. *Discuss. Faraday Soc.* **1951**, *11*, 125.
(10) Nierlich, M.; Williams, C. E.; Boue, F.; Cotton, J. P.; Daoud, M.; Farnoux, B.; Jannink, G.; Picot, C.; Moan, M.; Wolff, C.; Rinaudo, M.; de Gennes, P.-G. *J. Phys. (Paris)* **1979**, *40*, 701.
(11) Drifford, M.; Dalbiez, J.-P. *J. Phys. Chem.* **1984**, *88*, 5368.
(12) Katchalsky, A.; Michaeli, M. *J. Polym. Sci.* **1955**, *15*, 69.
(13) Katchalsky, A. *J. Polym. Sci.* **1959**, *12*, 159.
(14) de Gennes, P.-G.; Pincus, P.; Velasco, R. M.; Brochard, F. *J. Phys. (Paris)* **1976**, *37*, 1461.
(15) Pfeuty, P. *J. Phys., Collog.* **1978**, *39*, C2-149.
(16) Odijk, T. *Macromolecules* **1979**, *12*, 688.
(17) Joanny, J.-F.; Pincus, P. *Polymer* **1980**, *21*, 274.
(18) Khokhlov, A. R.; Khachaturian, K. A. *Polymer* **1982**, *23*, 1742.
(19) Witten, T. A.; Pincus, P. *Europhys. Lett.* **1987**, *3*, 315.
(20) Cates, M. E. *J. Phys. II (Paris)* **1992**, *2*, 1109.
(21) Odijk, T. *J. Polym. Sci., Polym. Phys. Ed.* **1977**, *15*, 477.
(22) Skolnick, J.; Fixman, M. *Macromolecules* **1977**, *10*, 944.
(23) Barrat, J.-L.; Joanny, J.-F. *Europhys. Lett.* **1993**, *24*, 333.
(24) Carnie, S. L.; Christos, G. A.; Creamer, T. P. *J. Chem. Phys.* **1988**, *89*, 6484.
(25) Christos, G. A.; Carnie, S. L.; Creamer, T. P. *Macromolecules* **1992**, *25*, 1121.
(26) Barenbrug, Th. M. A. O. M.; Smit, J. A. M.; Bedeaux, D. *Macromolecules* **1993**, *26*, 6864.
(27) Barrat, J.-L.; Boyer, D. *J. Phys. II (Paris)* **1993**, *3*, 343.
(28) Valleau, J. P. *Chem. Phys.* **1989**, *129*, 163.
(29) Christos, G. A.; Carnie, S. L. *J. Chem. Phys.* **1990**, *92*, 7661.
(30) Brender, C. *J. Chem. Phys.* **1990**, *93*, 2736.
(31) Le Bret, M. *J. Chem. Phys.* **1982**, *76*, 6243.
(32) Fixman, M. *J. Chem. Phys.* **1982**, *76*, 6346.
(33) Tricot, M. *Macromolecules* **1984**, *17*,. 1698.
(34) Khokhlov, A. R. *J. Phys. A* **1980**, *13*, 979.
(35) Manning, G. S. *J. Chem. Phys.* **1969**, *51*, 924.
(36) Le Bret, M.; Zimm, B. H. *Biopolymers* **1984**, *23*, 287.
(37) Bjerrum, N. *Z. Electrochem.* **1918**, *24*, 321.
(38) McQuarrie, D. A. *Statistical Mechanics*; Harper & Row: New York, 1976. Landau, L. D.; Lifshitz, E. M. *Statistical Physics*, 3rd ed.; Pergamon Press: New York, 1980; Part 1.
(39) de Gennes, P.-G. *Scaling Concepts in Polymer Physics*; Cornell University Press: Ithaca, NY, 1979.
(40) Borue, V. Yu.; Erukhimovich, I. Ya. *Macromolecules* **1988**, *21*, 3240.
(41) Joanny, J.-F.; Leibler, L. *J. Phys. (Paris)* **1990**, *51*, 545.
(42) Donnan, P. G.; Guggenheim, E. A. *Z. Phys. Chem.* **1934**, *162*, 364. Hill, T. L. *Discuss. Faraday Soc.* **1956**, *21*, 31; *J. Phys. Chem.* **1957**, *61*, 548.
(43) Wang, L.; Bloomfield, V. A. *Macromolecules* **1990**, *23*, 804.
(44) Stevens, M. J.; Kremer, K. *Phys. Rev. Lett.* **1993**, *71*, 2228.
(45) Rabin, Y.; Cohen, J.; Priel, Z. *J. Polym. Sci., Polym. Lett. Ed.* **1988**, *26*, 397.
(46) Cohen, J.; Priel, Z.; Rabin, Y. *J. Chem. Phys.* **1992**, *88*, 7111.
(47) Booth, F. *Proc. R. Soc. London* **1950**, *A203*, 533.
(48) Doi, M.; Edwards, S. F. *Theory of Polymer Dynamics*; Clarendon Press: Oxford, 1986.
(49) Colby, R. H.; Rubinstein, M.; Daoud, M. *J. Phys. II (Paris)* **1994**, *4*, 1299.
(50) Graessley, W. W. *Polymer* **1980**, *21*, 258.
(51) Kavassalis, T. A.; Noolandi, J. *Phys. Rev. Lett.* **1987**, *59*, 2674; *Macromolecules* **1989**, *22*, 2709.
(52) Lin, Y.-H. *Macromolecules* **1987**, *20*, 3080.
(53) Colby, R. H.; Rubinstein, M. *Macromolecules* **1990**, *23*, 2753.
(54) Koene, R. S.; Nicolai, T.; Mandel, M. *Macromolecules* **1983**, *16*, 231.
(55) Takahashi, A.; Kato, N.; Nagasawa, M. *J. Phys. Chem.* **1970**, *74*, 944.
(56) Nierlich, M.; Boue, F.; Lapp, A.; Oberthur, R. *J. Phys. (Paris)* **1985**, *46*, 649.
(57) Butler, J. A. V.; Robins, A. B.; Shooter, K. V. *Proc. R. Soc. London* **1957**, *A241*, 299.
(58) Ganter, J. L. M. S.; Milas, M.; Rinaudo, M. *Polymer* **1992**, *33*, 113.
(59) Fernandez Prini, R. F.; Lagos, A. E. *J. Polym. Sci., Part A* **1964**, *2*, 2917.
(60) Hodgson, D. F.; Amis, E. J. *J. Chem. Phys.* **1991**, *94*, 4581.
(61) Oostwal, M. G.; Blees, M. H.; de Bleijser, J.; Leyte, J. C. *Macromolecules* **1993**, *26*, 7300.
(62) Oostwal, M.; Odijk, T. *Macromolecules* **1993**, *26*, 6489.
(63) Kim, M. W.; Peiffer, D. G. *Europhys. Lett.* **1988**, *5*, 321.
(64) Tsimpris, C. W.; Suryanarayanan, B.; Mayhan, K. G. *J. Polym. Sci., Part A-2*, **1972**, 10, 1837.
(65) Yamaguchi, M.; Wakatsu, M.; Takahashi, Y.; Noda, I. *Macromolecules* **1992**, *25*, 470, 475.
(66) Noda, I.; Takahashi, Y. *Polym. Prep. (Am. Chem. Soc., Div. Polym. Chem.)* **1994**, *35*, 154.
(67) Rubinstein, M.; Colby, R. H.; Dobrynin, A. V. *Phys. Rev. Lett.* **1994**, *73*, 2776.
(68) Tam, K. C.; Tiu, C. *J. Non-Newtonian Fluid Mech.* **1993**, *46*, 275.
(69) Nyrkova, I. A.; Shusharina, N. P.; Khokhlov, A. R. *Polym. Prepr. (Am. Chem. Soc., Div. Polym. Chem.)* **1993**, *34* (1), 939.

MA9412849